

Image Processing of Mammograms for Breast Cancer ROI Identification

Caitlin Hansen, Paul Klaucke

Department of Computer Science

Southern Connecticut State University

New Haven, CT, 06515, USA

Abstract—Mammography, specialized x-ray imaging for scanning the breasts, is the clinically accepted imaging modality used for early detection and diagnosis of breast cancer [1]. Currently, interpretations of mammograms follow standardized guidelines set forth by the American College of Radiology (ACR) in a system called BI-RADS (Breast Imaging Reporting and Database System). This system is used by radiologists to classify abnormal features, including microcalcifications, masses, bilateral asymmetry, and architectural distortion [2]. In this paper, the authors implement an algorithm to extract mammogram regions of interest (ROIs) and test three methods of segmentation: thresholding based on max intensity value (Method A), k-means clustering (Method B), and Otsu's method of thresholding (Method C). Classified mammogram images from the mini-MIAS Database with confirmed malignant characteristic regions were tested. ROI extraction was performed by (1) removing background artifacts and pectoral muscle tissue from the mammogram, (2) enhancing the image using Contrast-Limited Adaptive Histogram Equalization, (3) segmenting the image, (3) applying morphological operations, and (4) overlaying the extracted ROI on the original image for visual inspection. To demonstrate capability of the proposed methodology, experimental results were compared to corresponding BI-RADS classifications.

I. INTRODUCTION

BREAST cancer is the most frequently occurring cancer in women and poses a major public health problem. The American Cancer Society reports that currently one in eight women in the United States will develop breast cancer in her lifetime. By the year 2050, the worldwide incidence of female breast cancer is predicted to reach approximately 3.2 million new cases per year. In terms of its etiology and pathological characteristics, breast cancer is highly varied from patient to patient, making both the diagnosis and prognosis difficult to both classify and standardize.

Breast cancer is a disease in which malignant cells form in the tissues of the breast. Currently, digital mammograms are the most effective imaging modality used for early detection and diagnosis of abnormal breast features [1]. Digital mammography uses low dose x-rays combined with an electronic x-ray detector to convert the image into a digital picture. The x-ray detector measures penetration of radiation through tissue, or the degree to which tissue attenuates x-rays. Since attenuation is determined by tissue type and distribution, images are highly useful for breast cancer diagnosis. The clinical mammogram image convention is to display attenuated radiation as white.

Highly attenuating structures include glands, connective tissue, and abnormalities. Less dense tissue, such as fat, appears darker in images. Images can be further processed with digital mammography by altering the magnification, orientation, brightness, and contrast to increase clarity in regions of interest. Despite this image enhancement, the American Cancer Society reports that about one in five incidences of breast cancer are missed by mammography. One of the major difficulties posed to radiologists using mammograms to diagnose breast cancer is the large variation in the proportion of fibrous connective tissue and glandular tissue to fatty tissue breast density among individuals. This large variation in breast density convolutes visibility of tissue abnormalities such as lesions, masses, calcifications, architectural distortion, and bilateral asymmetries. [2].

Currently, interpretations of mammograms follow standardized guidelines set forth by the American College of Radiology (ACR) in a system called BI-RADS (Breast Imaging Reporting and Database System). This system is used by radiologists when reviewing mammograms to both describe breast density and classify abnormal features [2]. Breast density is divided into four tissue categories: fat tissue, scattered fibroglandular dense tissue, heterogeneously dense tissue, and extremely dense tissue. As the density of the breast increases, the sensitivity of the mammography imaging decreases, increasing the likelihood of a false-negative diagnosis of breast cancer.

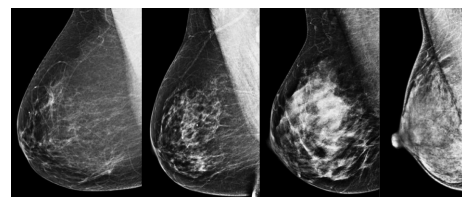


Fig. 1. From left to right: Fat tissue, fibroglandular tissue, heterogeneously dense tissue, extremely dense tissue

Furthermore, BI-RADS defines mammographic features of concern including masses, calcifications, architectural distortion, and bilateral asymmetry. Each mammogram is given an assignment of a categorical value of zero through six based on the mammographic features as the following: 0 = incomplete, 1 = negative, 2 = benign, 3 = probably benign, 4 = suspicious, 5

= highly suggestive of malignancy, and 6 = proven malignancy [3]. Radiologists give higher ratings to calcifications with dimensions of 0.2 to 0.3 mm and to aligned or clustered microcalcifications. Bilateral asymmetry is an asymmetry of the breast parenchyma between the left and right breast. An architectural distortion is a disruption of the normal, randomly distributed curvilinear and fine linear radio plaque structures, presenting no visible mass [7].

II. RELATED WORK

Many studies have undertaken the difficult task of image processing mammograms. At a minimum, these studies have attempted to simplify a medical professional's difficult task of mammogram analysis by denoising images [1] and [5], outlining the breast contour [1], and passively enhancing visibility of abnormal tissue features. Both [1] and [5] apply similar enhancement techniques of double thresholding segmentation by manually selecting a lower and upper bound and then applying morphological operations. Both of these studies produced contrast enhanced images, but did not compare the outcome to ground truth values. Consequently, the accuracy of the proposed algorithms was not assessed. More ambitious studies have gone a step further by actively enhancing and delineating abnormal tissue [5], [7], and [8]. Due to the complexity and wide variation of the tissue structure represented across multi-patient mammogram images, these studies generally perform an analysis on a single or small subset of images ($n < 10$) [6], [1], [5], effectively over-training and ensuring algorithm "success". Consequently, there is a disparity of robust mammogram processing algorithms that can both enhance and autonomously delineate ROIs across a diverse range of tissue types including fatty, dense, and glandular breast tissue.

In this paper, the authors develop and implement an algorithm to enhance abnormal breast features in images. Three different segmentation techniques were tested: k-means clustering, Otsu's method of thresholding, and finally thresholding based on the max intensity of the Gaussian smoothed image. The authors compared output ROIs to "ground truth" ROIs delineated in the Mammographic Image Analysis Society (MAIS) mini-database of digital mammograms. These images include radiologist "truth" markings on the locations of any abnormalities that may be present in the images as well as tabulation of breast density that can be compared to BI-RADS assessment guidelines.

III. PROPOSED METHODOLOGY

This section discusses image cropping, pre-processing, segmentation, morphological operations, and comparison with ground truth ROIs. Three different segmentation methods were tested using the same pre-processing and morphological operations and the success of each segmentation method was evaluated. Method A set a threshold value based on the max intensity of the Gaussian smoothed image, Method B used k-means clustering with 10 clusters, and Method C used Otsu's method of thresholding. The general flow chart

of the methodology is shown in Figure 2. For each of the steps in the proposed methodology, a single representative mammogram image was used to demonstrate the input and output result for this paper.

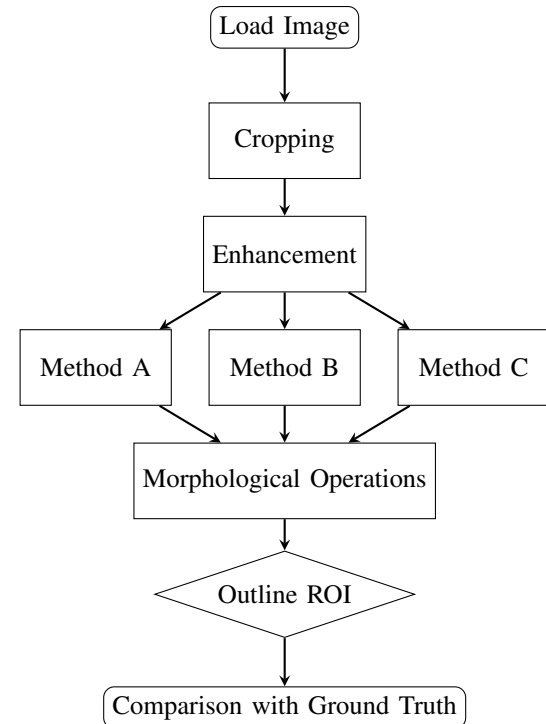


Fig. 2. Block diagram of proposed method. Method A, B, and C represent the three different segmentation methods of setting a threshold: thresholding based on max smoothed image intensity values, k-means clustering, and Otsu's method, respectively.

A. Cropping - Removing Background and Muscle Tissue

Mammogram x-rays are often taken with a label present to help radiologists identify the type of image. Image artifacts such as labels (Fig. 31) may interfere with image processing. Therefore, an initial step in image processing is to remove the artifacts from mammogram images. Furthermore, the American College of Radiology distinguishes between tumors of pectoral muscle tissue and tumors of breast tissue as chest wall cancer and breast cancer, respectively. Since the pectoral muscle region of mammograms appear as bright spots of similar intensity to cancerous regions of the breast, this study also removed the pectoral region of the mammogram. Removal of both the pectoral region and label is shown in Figures 3 and 4.

Representative Mammogram Cropping

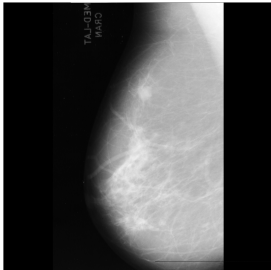


Fig. 3. Original mammogram from mini-MIAS database

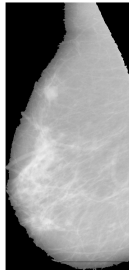


Fig. 4. Removed background and muscle tissue

B. Pre-Processing - Enhancement

The resulting images were then enhanced using Contrast-Limited Adaptive Histogram Equalization (CLAHE). This process enhances the contrast of the image by transforming the intensity values by operating on small data regions, called tiles, and then combining neighboring tiles through bilinear interpolation. Over-amplification of noise in homogeneous areas of the input image is greatly reduced. This result differs from normal histogram equalization, which in contrast is applied to the entire image.

Representative Mammogram Enhancement

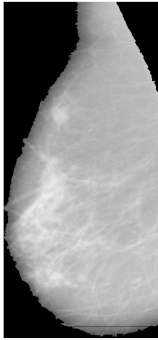


Fig. 5. Cropped image

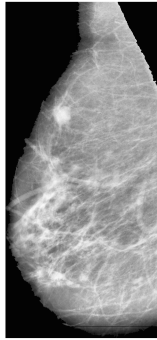


Fig. 6. Enhanced image

C. Segmentation

1) Method A: Segmentation Based on Max Intensity Pixel Value: The images were first smoothed by convolution with a 2D Gaussian smoothing kernel, or mask, with a standard deviation of 1.

$$G(x, y) = \frac{1}{2\pi\sigma^2} e^{-\frac{x^2+y^2}{2\sigma^2}} \quad (1)$$

In this equation, x and y represent the pixel location and σ represents one standard deviation. Convolution is the process of moving a mask that is rotated 180 degrees across an image while summing the products at each pixel location in the image.

The threshold level was set equal to 80 percent of the max intensity value in the smoothed image. This method

was chosen because it dynamically adapts to each image, instead of using a static threshold that will yield different results for a high vs low contrast image. For dense breast tissue, a higher threshold of 85 percent of the max smoothed intensity value was used, since normal breast tissue in this case exhibited lower contrast with the abnormal tissue. A representative mammogram showing the output of this segmentation technique is shown in Figure 7 and 8.

Representative Mammogram Method A Segmentation

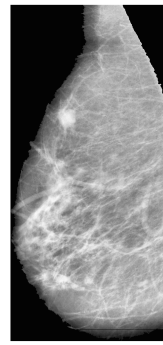


Fig. 7. Original mammogram from mini-MIAS database

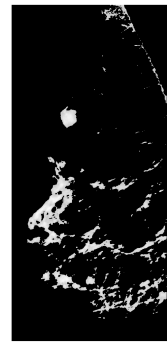


Fig. 8. Method A Segmentation

2) Method B: Segmentation Based on K-Means Clustering:

K-means clustering randomly selects centroid locations in a data set. The sum of the squared distance between datapoints and centroids is calculated using equation 3. Next, each datapoint value is assigned to the closest centroid location. The value m_k represents the average of all the datapoints belonging to that cluster. This processes is repeated until the centroid locations reach convergence and no datapoint assignments change. Then the centroid for the cluster is found by averaging all the datapoints that belong to that cluster using equation 2. Note that the dimensionality of the data can vary– for an RGB image the centroid will be found in 3D space. For a grayscale image, it will be found in 1D.

$$E = \sum_{k=1}^K \sum_{x \in C_k} d^2(x, m_k) \quad (2)$$

$$d^2(x, m_k) = \sum_{n=1}^N (x_n - m_{kn})^2 \quad (3)$$

The k-means algorithm was applied to segment the images using ten clusters. This number of clusters was chosen because it was sensitive enough to differentiate the high pixel intensity values corresponding to tumors from other high intensity (dense) tissue values. Figure 9 represents four of the ten clusters corresponding to the first (a), fourth (b), seventh (c), and the tenth (d) cluster centroid values. The highest intensity cluster was used for ROI segmentation prior to morphological operations for Method B. A representative mammogram showing the output of this segmentation technique is shown in Figures 10 and 11.

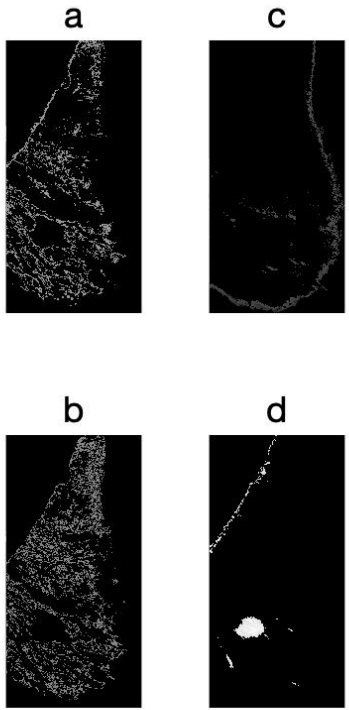


Fig. 9. Images (a), (b), (c), and (d) correspond to the minimum, fourth, seventh, and maximum value cluster centroids, respectively. Image (d) shows the cluster containing the ROI.

Representative Mammogram Method B Segmentation

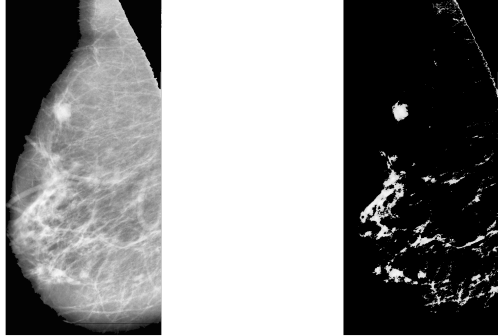


Fig. 10. Enhanced image

Fig. 11. Method B segmentation

3) Method C: Segmentation Based on Otsu's Method: For this method, the images were thresholded using Otsu's method to make the images binary. When an image is properly thresholded, the average error incurred in separating pixels to differing groups, referred to as classes, should be minimized. Otsu's method of thresholding maximizes the between class variance, thus minimizing the average error in the assignment of classes. For this method, the accuracy of a threshold level is assessed by comparing the ratio of the global variance σ_G^2 to the between class variance σ_B^2 .

$$\eta = \frac{\sigma_B^2}{\sigma_G^2} \quad (4)$$

where

$$\sigma_B^2 = P_1 (m_1 - m_g)^2 + P_2 (m_2 - m_g)^2 \quad (5)$$

and

$$\sigma_G^2 = \sum_{i=0}^{L-1} (i - m_g)^2 p_i \quad (6)$$

Here, m_1 is the mean intensity value of pixels assigned to class 1, m_g is the global mean intensity value of the entire image, m_2 is the mean intensity value of pixels assigned to class 2, P_1 is the probability that a pixel is assigned to class 1, P_2 is the probability that a pixel is assigned to class 2, and p_i is the number of pixels of a specific intensity divided by the total number of pixels in the image. This segmentation technique output can be seen in 12 and 13.

Representative Mammogram Method C Segmentation

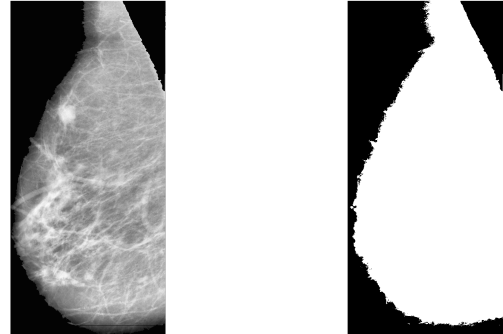


Fig. 12. Enhanced image

Fig. 13. Method C segmentation

D. Morphological Operations

The same morphological operations were applied to process the resulting binary images following Methods A, B, and C. A structuring disk with radius of 13 pixels was used to probe the input images. The structuring shape was chosen as a disk because ground truth ROI's are defined in the mini-MIAS database by an x and y image coordinate and a radius in pixels. The radius size of 13 was chosen because in the mini-MIAS database, the smallest malignant tumor identified had a radius of 14 pixels. Therefore, it is assumed that any features with a radius of less than 14 pixels are not malignant tumors. Figure 14a simulates a mammogram image structure that is less than the minimum malignant tumor size. Figure 14b shows the result of opening Figure 14a with a structuring disk of radius 13 pixels. Since the structuring element is the same size as the image feature, the feature is removed after image opening. Figure 14c simulates an image feature as a disk of radius 14 pixels. Image opening 14c with a disk of radius 13 preserves the feature as seen in 14d.

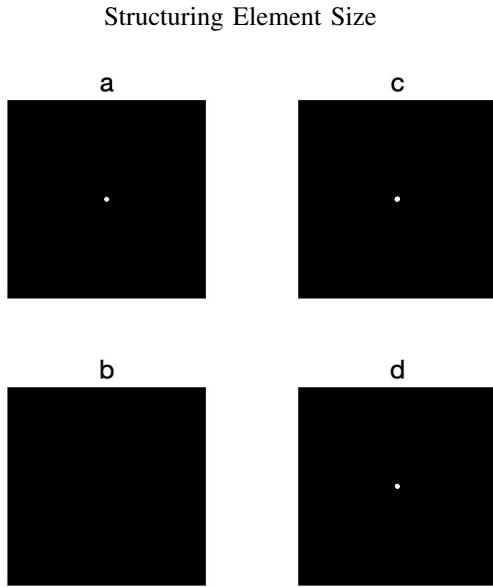


Fig. 14. The images shown in (a-d) above simulate that using a structuring element of size 13 is successful in eliminating pixel regions with diameters less than 14 pixels. Image (a) shows a disk region of radius 13 pixels and (b) shows a disk region of radius 14 pixels. A structuring element of a disk shape with radius 13 was applied to both (a) and (c) and the output is shown in (b) and (d), respectively. For (c) the original object in (a) is removed and for (d) the original object in (b) is preserved. This validates the decision to base the structuring element as a disk of radius 13 to preserve the minimum tumor size listed in the mini-MIAS database.

Morphological opening was performed, which consists of an erosion followed by a dilation, using the same disk structuring element. The dilation of the input image A, by the structuring element B, is defined as

$$A \oplus B = \{(x, y) + (u, v) : \epsilon A, (u, v) \in B\} \quad (7)$$

The input image A is translated by every point in B and the union of the results are taken. The erosion of the input image, A, by the structuring element, B, is defined as

$$AB = \{w : B_w \subseteq A\} \quad (8)$$

To perform an erosion, the structuring element, B, is translated over A and for each place that all points of B fit into A, the corresponding (0,0) point of B is recorded. This process is iterated so that all points that satisfy these conditions form the erosion. This process is shown in Figures 15 and 16.

Representative Mammogram Morphological Operations

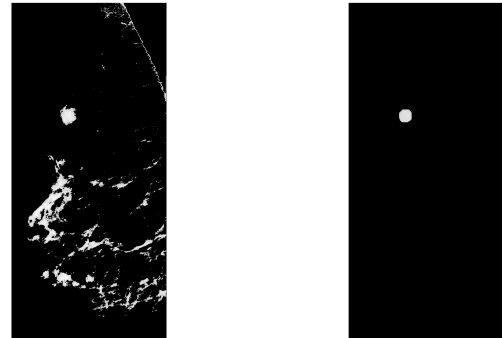


Fig. 15. Segmented image

Fig. 16. Morphological operations

E. Overlaying the Extracted ROI Outline

To get the outlines of the ROIs and then subsequently overlay these outlines on to the original images, the perimeter of the ROIs (binary images) were first identified. Perimeter pixels were determined to be those that were both nonzero and connected to at least one zero-valued pixel. This step produced black and white outlines of the ROIs. To improve visibility of the outlines, a dilation was performed to thicken the outlines. The outline was converted to an RGB image and the output ROIs were colored red. These outlines were then overlaid on the cropped images as outlined in subsection III A. Figures 17 and 18 show the input and output of this step.

Overlaying the Extracted ROI

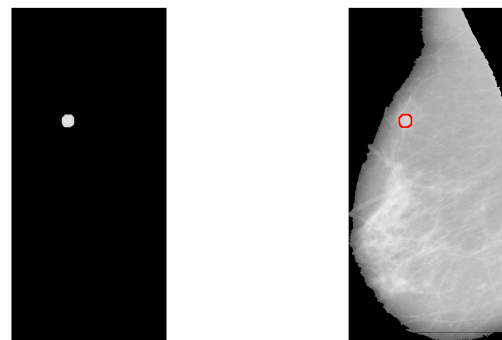


Fig. 17. Morphological operations

Fig. 18. Overlaying extracted ROI

F. Truth Region Identification and Data Set

In the mini-Mias database, ground-truth tumor ROIs were documented with a pixel location and a radius value. To overlay this region on the original images, a disk was created in a binary image at the correct location and with the correct radius. The disk perimeter was extracted and overlaid on the original images. The color of the perimeter was changed to blue as shown in Figures 19 and 20. User access to the database can be found in [4].

Representative Mammogram Truth Region Identification

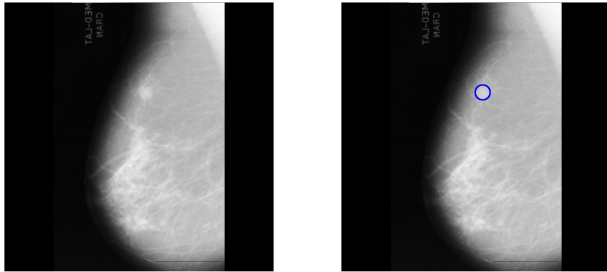


Fig. 19. Original mammogram from mini-MIAS database before any processing.

Fig. 20. Outlined truth ROI as provided by the mini-MIAS database. The blue outline represents the known cancerous region.

IV. RESULTS AND DISCUSSION

The variation in breast tissue density across mammogram images made it difficult to generate an algorithm that was successful in identifying ROIs for all tissue types. For this study, ROI delineation was deemed successful if the study ROI and ground truth ROI (defined by the mini-MIAS database) overlapped. Visual inspection of the output image was used to determine success or failure. In some cases, the study ROI was slightly larger or more disperse than the ground truth ROI (Fig. 32). In other cases, the study ROI overlapped with the ground-truth ROI, but the study ROI was too large, incorrectly shaped, or was comprised of many different image regions (Fig. 21). These ROIs were counted as a failure.

Example of Failure with Multiple ROIs

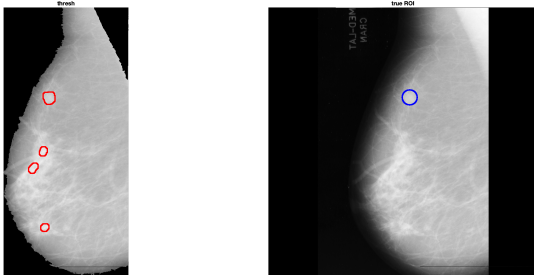


Fig. 21. Post-processing with multiple ROIs identified.

Fig. 22. Ground truth showing only a single ROI.

Of the three segmentation methods tested, Method A proved to have the highest overall success rate. Method A had a success rate of identifying malignant tumors of 72.22% for fatty tissue, 68.75% for glandular tissue, and 29.41% for dense tissue. Method B had a success rate of 50.00% for glandular tissue, 44.44% for fatty tissue, and 29.41% for dense tissue. Method C did not successfully identify ROIs in any type of breast tissue. It is difficult to compare the results of this study to previous studies because methods tested in previous studies did not include a large comprehensive data set that included a wide range of tissue types.

TABLE I
METHOD A: SUCCESS FOR VARIOUS TISSUE TYPES WITH KNOWN MALIGNANT TUMORS

	Dense	Glandular	Fatty
Successful Images	5	11	13
Total Images	17	16	18
Success Rate	29.41%	68.75%	72.22%

TABLE II
METHOD B: SUCCESS FOR VARIOUS TISSUE TYPES WITH KNOWN MALIGNANT TUMORS

	Dense	Glandular	Fatty
Successful Images	5	8	8
Total Images	17	16	18
Success Rate	29.41%	50.00%	44.44%

TABLE III
METHOD C: SUCCESS FOR VARIOUS TISSUE TYPES WITH KNOWN MALIGNANT TUMORS

	Dense	Glandular	Fatty
Successful Images	0	0	0
Total Images	17	16	18
Success Rate	0.00%	0.00%	0.00%

Method C, the Otsu method, was unsuccessful across all types of mammograms because the intensity values of ROIs in mammograms are very similar to the intensity values of the surrounding tissue. Since the Otsu method of thresholding will binarize the image into classes based on a division that maximizes the between class variance, it will not separate out the bright ROIs. For example, the histogram, Figure 23, for a representative mammogram image after enhancement displays a bimodal distribution where the dark intensity values are the black background of the mammogram and the lighter represent the breast tissue. The brightest pixels will represent an ROI, but the Otsu method will group these pixels into a class that includes bright pixels corresponding to normal, dense breast tissue. For mammogram ROI identification, a thresholding method must be more sensitive to peaks in the highest intensity region of the histogram. It appears that the Otsu method of thresholding sets threshold levels too low to segment these high pixel values, as apparent in Figures 24 and 25. This mammogram is representative of the outcome of all the mammograms despite tissue type; the outlined region included the ROIs along with other high intensity pixel values corresponding to healthy tissue.

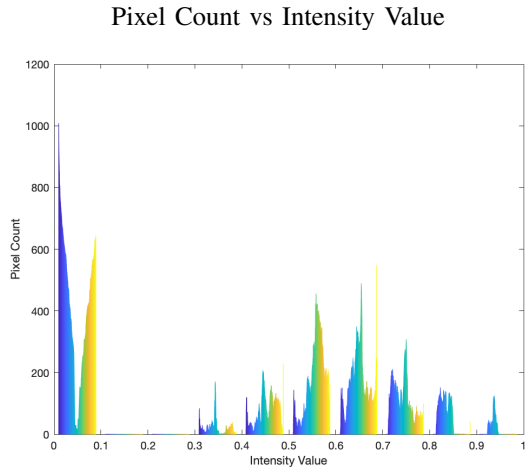


Fig. 23. Histogram corresponding to 24 enhanced mammogram. The highest intensity peak represents the ROI in the image, but the Otsu method will group that peak with other high intensity pixel values belonging to other regions of breast tissue in order to maximize the between class variance.

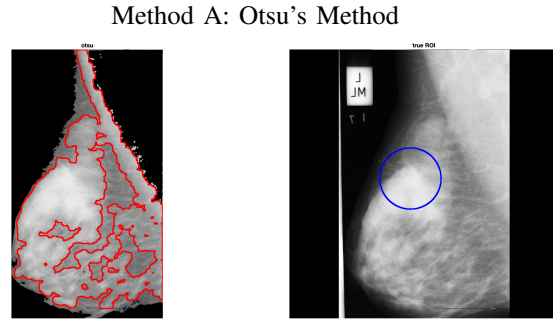


Fig. 24. Post-Processing fatty tissue. The Otsu method did not set a high enough threshold level to delineate the true ROI.

Fig. 25. Ground truth fatty tissue.

Method A proved to be the optimal method because it accounted for the wide variation in tissue density among breasts and the resulting variation in contrast between the images. Since malignant tumors attenuate radiation more so than healthy tissue, ground truth ROIs appear brighter in mammogram images than other tissue. This method was the most successful at thresholding the images because it was based off of the max smoothed intensity pixel value of each individual image. This allowed for higher adaptability across a wide variety of mammogram images compared to the other methods tested and better segmentation of high intensity pixel values. Figures 26 through 31 show the high accuracy of this method across the range of tissue types.

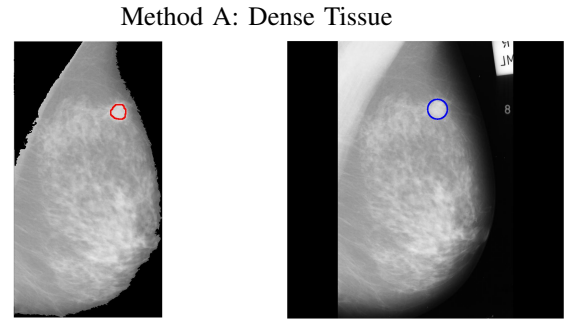


Fig. 26. Post-processing dense tissue.

Fig. 27. Ground truth dense tissue.

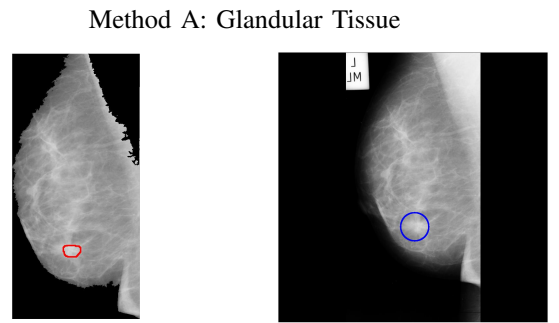


Fig. 28. Post-processing glandular tissue.

Fig. 29. Ground truth glandular tissue.

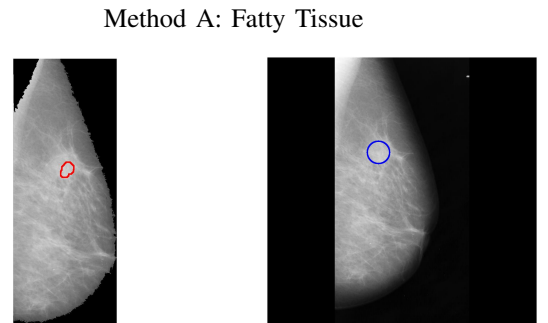


Fig. 30. Post-processing fatty tissue.

Fig. 31. Ground truth fatty tissue.

Method B, using k-means segmentation, was less successful on fatty and glandular tissue types than Method A. This result is likely because the wide variation in contrast across mammograms meant having a static number of clusters (10 clusters was used in this study) did not apply universally across all the images. Dynamically adjusting the cluster size based on image contrast could be a way of improving this segmentation method. Furthermore, because the centroids are chosen randomly each time the algorithm is run, it is possible that future runs of the same images will output different results. For this study, however, these differences were not large enough to produce a significant change in the outcome of the results.

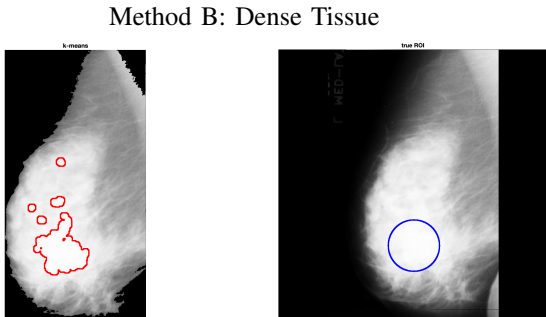


Fig. 32. Post-Processing

Fig. 33. Ground truth dense tissue.

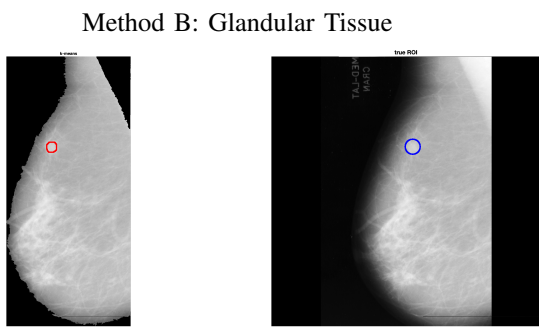


Fig. 34. Post-processing glandular tissue.

Fig. 35. Ground truth glandular tissue.

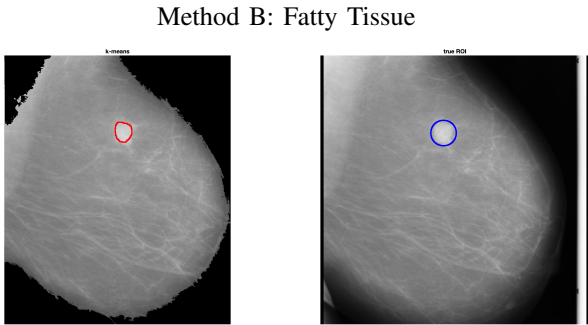


Fig. 36. Post-processing fatty tissue.

Fig. 37. Ground truth fatty tissue.

As noted in previous studies [2] and [5], identification of tumors in dense breast tissue using mammograms is difficult. Overall, all three segmentation methods were less successful at identifying ROIs in dense breast tissue, presumably due to reduced contrast between tissue and tumors in dense tissue compared to the contrast in fatty or glandular tissue. The histograms of mammograms with dense tissue have peaks located at higher intensity values that are left skewed while the histograms of mammograms with fatty tissue have peaks at lower intensity values that are more symmetric. For example, the histogram for Figure 32 and the histogram for Figure 36 are shown below in Figures 38 and 39, respectively. In the histogram corresponding to the dense breast tissue mammogram (Fig. 38), a much larger portion of the image is comprised of high intensity values, so differentiating harmful ROIs from benign ones.

Pixel Count vs Intensity for Dense Tissue

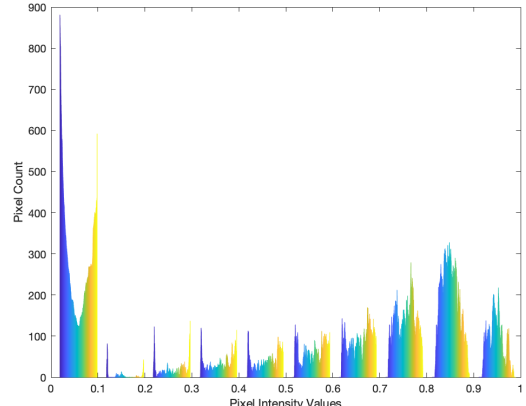


Fig. 38. Histogram corresponding to Figure 32: a dense tissue mammogram. The data displays a left skewed peak at the intensity value of .85.

Pixel Count vs Intensity for Fatty Tissue

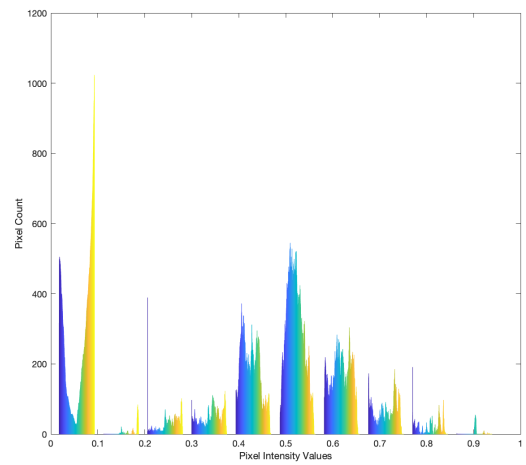


Fig. 39. Histogram corresponding to Figure 36: a fatty tissue mammogram. The data displays a symmetric peak at the intensity value of .5.

between healthy and unhealthy tissue is more difficult. In Figure 39 a very small portion of the image is represented by the peak intensity values, so segmentation is more effective.

It is worth noting that the algorithms applied in this study will detect ROIs regardless of whether or not a subject has breast cancer. If this was to be implemented in a clinical setting to aid radiologists in detection of breast cancer in mammogram images, the defined ROIs could be representative of benign tumors, calcifications, or other high contrast regions that are not actually representative of cancer. Deep learning could be a potential means of differentiating harmful ROIs from benign ones.

V. CONCLUSIONS AND FUTURE WORK

Breast cancer is a significant world health issue as it is the most frequency occurring cancer in women. Early detection is essential to prognosis, but the poor contrast in

mammograms results in 1 out of 5 cancers going undiagnosed in mammogram screenings. While completely autonomous computer tumor identification may one day be feasible, a more realistic goal is to aid physicians in identifying abnormal tissue in mammograms using the methods outlined in this study. This could help reduce the number of false-negatives following mammogram analysis in a clinical setting. For this study, three segmentation methods for malignant tumor ROI identification in mammograms were developed and tested: thresholding based on the max smoothed pixel intensity value (Method A), K-means clustering (Method B), and Otsu's method (Method C). Following each method, a final step of morphological image processing was applied, in which a final ROI was delineated. The most successful method was thresholding based on the max smoothed intensity pixel value. K-means clustering segmentaiton was slightly less successful, and the Otsu method yielded a zero rate of success for all tissue types. Tumor ROI identification was most successful for fatty breast tissue, with dense tissue yielding the lowest rate of success due to lower healthy-abnormal tissue contrast.

Future studies should focus on improving the detection of ROIs in dense tissue mammograms as these mammograms proved to be the most difficult to accurately segment. Although this study focused on segmentation techniques for thresholding the images, future studies should evaluate enhancement techniques prior to segmentation. By improving the contrast in dense tissue mammograms, the segmentation technique applied can be further optimized. Additionally, an ROI success metric should be determined so that the success or failure of an ROI identification is not subjective. Furthermore, future studies could evaluate geometric characteristics of the ROIs to look for common characteristics in malignant ROIs. This would aid radiologists in identifying these ROIs as benign or malignant.

REFERENCES

- [1] BADAWY, S. M., HEFNAWY, A. A., ZIDAN, H. E., AND GADALLAH, M. T. Breast cancer detection with mammogram segmentation: a qualitative study. *International Journal of Advanced Computer Science and Application* 8, 10 (2017).
- [2] BOZEK, J., DELAC, K., AND GRGIC, M. Computer-aided detection and diagnosis of breast abnormalities in digital mammography. In *2008 50th International Symposium ELMAR* (2008), vol. 1, IEEE, pp. 45–52.
- [3] BURNSIDE, E. S., SICKLES, E. A., BASSETT, L. W., RUBIN, D. L., LEE, C. H., IKEDA, D. M., MENDELSON, E. B., WILCOX, P. A., BUTLER, P. F., AND D'ORSI, C. J. The acr bi-rads® experience: learning from history. *Journal of the American College of Radiology* 6, 12 (2009), 851–860.
- [4] CLARK, A. The mini-mias database of mammograms.
- [5] KADHIM, D. A. Development algorithm-computer program of digital mammograms segmentation for detection of masses breast using marker-controlled watershed in matlab environment. *journal of kerbala university* 1, (2012), 114–123.
- [6] NAGI, J., KAREEM, S. A., NAGI, F., AND AHMED, S. K. Automated breast profile segmentation for roi detection using digital mammograms. In *2010 IEEE EMBS conference on biomedical engineering and sciences (IECBES)* (2010), IEEE, pp. 87–92.
- [7] PARAMKUSHAM, S., RAO, K., AND RAO, B. Early stage detection of breast cancer using novel image processing techniques, matlab and labview implementation. pp. 1–5.
- [8] SUHAIL, Z., SARWAR, M., AND MURTAZA, K. Automatic detection of abnormalities in mammograms. *BMC medical imaging* 15, 1 (2015), 53.